

Structural, transport and infrared studies of oxidic spinels $Zn_{1-x}Ni_xFeCrO_4$

S. AL DALLAL, M. N. KHAN, ASHFAQ AHMED
Department of Physics, University of Bahrain, Bahrain, Arabian Gulf

X-ray, electrical conductivity and IR studies for the system $Zn_{1-x}Ni_xFeCrO_4$ were carried out. All the compounds, $0 \leq x \leq 1$ showed cubic symmetry. X-ray intensity calculations and IR studies indicate the presence of Zn^{2+} at tetrahedral sites, Ni^{2+} and Cr^{3+} at octahedral sites, and Fe^{3+} ions are equally distributed at both the sites. Activation energy and thermoelectric coefficient decreases with the increasing values of x . All the compounds exhibit P-type semiconductivity which may be due to transfer of Fe^{3+} ions from B-site to A-site creating holes. The electrical resistivity temperature behaviour obeys the relation $\rho = \rho_0 \exp(\Delta E/kT)$. The mobility of holes as calculated from IR and conductivity data is of the order of $10^{-9} \text{ cm}^2 \text{ V sec}^{-1}$. The probable ionic configuration for the system is suggested to be $Zn_{1-x}^{2+} Fe_x^{3+} [Fe_{1-x}^{3+} Ni_x^{2+} Cr^{3+}] O_4^{2-}$.

1. Introduction

Oxidic spinels (AB_2O_4) type find technological as well as commercial applications as catalyst, magnetic materials, thermistors etc. [1-3]. The electrical and magnetic properties of spinel oxides are controlled by oxidation states and location of cations at the tetrahedral (A) and octahedral (B) sites in the lattice. The so-called cation distribution depends on many factors such as temperature, pressure, composition and also on the method of preparation of the compounds [4-6]. We have earlier reported our results on oxidic spinel systems $ZnFeCrO_4$ and $NiFeCrO_4$ [7] $Zn_{1-x}CO_xMn_{1-x}Fe_xCrO_4$ [8] and $CO_{2-x}Ti_{1-x}Mn_{2x}O_4$ [9] prepared by conventional ceramic methods. The present studies were carried out in order to elucidate the structural, electrical and spectroscopic properties of the system $Zn_{1-x}Ni_xFeCrO_4$ prepared by a new coprecipitation technique.

2. Experimental procedure

2.1. Sample preparation

Samples of the system $Zn_{1-x}Ni_xFeCrO_4$ were prepared by a new coprecipitation technique. The starting materials were analytical reagent grade soluble chlorides $ZnCl_2 \cdot 6H_2O$; $NiCl_2 \cdot 6H_2O$; $FeCl_3 \cdot 6H_2O$ and $CrCl_3 \cdot 6H_2O$, used to obtain Zn^{2+} , Ni^{2+} , Cr^{3+} and Fe^{3+} ions in aqueous solution. An aqueous solution containing these ions in the required molar proportions was prepared by dissolving the above salts in stoichiometric proportions in distilled water. It was then precipitated by adding sodium hydroxide and pH of the solution was maintained between 9.00 and 9.50. The solution was kept on the water bath maintained at 80°C for 3 h and then oxidised by adding 75 ml to 80 ml of 30% (100 vol) of H_2O_2 dropwise with constant stirring until precipitation was complete. After the reaction was over, the resultant precipitate was filter washed with

distilled water to remove excess of sodium hydroxide. It was then dried at 80°C in a vacuum cryostat for 2 h. The dry precipitate was ground and made into pellets using polyvinyl acetate as a binder and heated at 900°C for 8-10 h. The pellets were ground into fine powder and made into pellets again and sintered at 1000°C for 5 h when single phase spinels were formed. This single phase formation was confirmed by X-ray diffraction patterns. The composition of the product was checked by chemical analysis.

2.2. Structural analysis

X-ray powder diffraction patterns were recorded on a diffractometer (Siemens D-500, Krista Uoflex) with a microprocessor controller, using $CuK\alpha$ radiation ($\lambda = 0.15405 \text{ nm}$) with a Ni filter. The X-ray patterns of all the compositions indicate the formation of a single spinel phase. To measure the intensity, the areas under different (hkl) peaks were determined and values obtained in relation to the peaks area for the 311 reflection which is taken to represent 100. To calculate the relative integrated intensity, I of a given (hkl) reflection, the following formula suggested by Buerger [10] is used where notation has its usual meaning:

$$I = [F_{hkl}]^2 P(1 + \cos^2 2\theta) / (\sin^2 \theta \cos \theta) \quad (1)$$

The atomic scattering powers for various ions are taken from literature [11]. To determine the cation distribution and its variation with the composition, the intensity ratios (I_{220}/I_{400} , I_{220}/I_{440} and I_{440}/I_{422}) for different possible models of cation distribution are calculated for the reflections 220, 400, 422 and 440 which are sensitive to cation distribution at both sites [12]. These were then compared with the observed intensity ratios. The maximum standard deviation in the observed ratios was ± 0.02 .

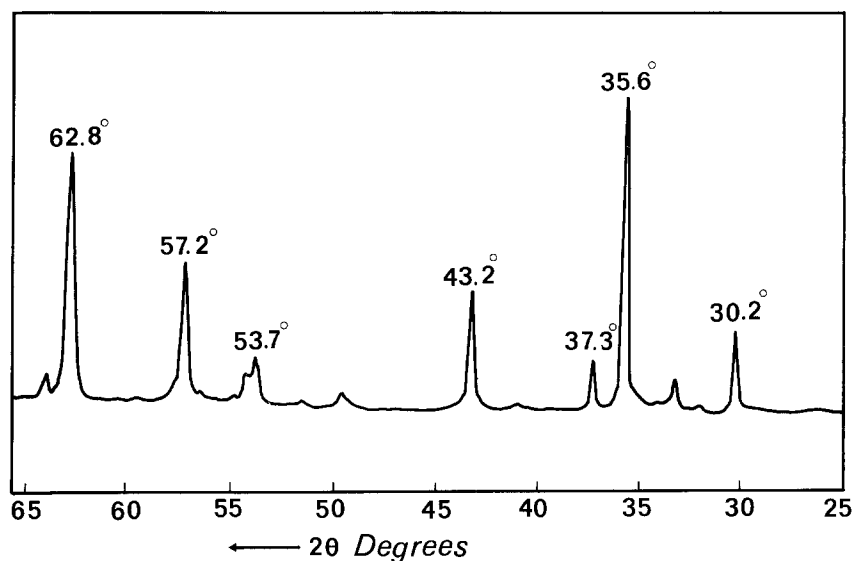


Figure 1 X-ray diffractogram for the system $\text{Zn}_{0.5}\text{Ni}_{0.5}\text{FeCrO}_4$.

2.3. Transport studies

The d.c. conductivity and thermoelectric power measurements were carried out using the techniques described elsewhere [13]. An LCR Marconi bridge with two probe conductivity arrangement was used. The end face of each pellet was coated with a thin layer of conducting silver paste and all measurements were carried out in the temperature range 300–623 K. The thermoelectric coefficient was measured from room temperature to 437 K by sandwiching a thick pellet between two copper blocks. The temperature differences across the sample were measured using a copper constantan thermocouple and the potential difference generated was measured using a micrometer.

2.4. Infrared spectra

The IR spectra were recorded at room temperature on a Perkin-Elmer infrared spectrophotometer in the range 200–4000 cm^{-1} .

3. Results and discussion

3.1. Structural analysis

Figure 1 shows the X-ray diffractogram of the compound $\text{Zn}_{0.5}\text{Ni}_{0.5}\text{FeCrO}_4$. The results of X-ray analysis are given in Table I. It is found that all compounds of the system $\text{Zn}_{1-x}\text{Ni}_x\text{FeCrO}_4$ are cubic in the range $0 \leq x \leq 1$. The lattice constant decreases from ZnFeCrO_4 ($a = 0.8393$ nm) to NiFeCrO_4 ($a = 0.835$ nm). The compound ZnFeCrO_4 crystallizes in cubic symmetry with ($a = 0.8393$ nm). This value agrees with the value ($a = 0.8388$ nm) reported by Les [14]. The decrease of the lattice constant is due to the replacement of larger Ni^{2+} ion by comparatively smaller Fe^{3+} ion in the tetrahedral site [15]. The cation distribution at A- and B-sites in the system was obtained by X-ray intensity calculations. The observed and calculated intensity ratios for the compound $\text{Zn}_{0.5}\text{Ni}_{0.5}\text{FeCrO}_4$ and ZnFeCrO_4 are summarized in Table II. It is seen that the model with Zn^{2+} at A-site; Ni^{2+} and Cr^{3+} at B-site and Fe^{3+} equally distributed between A- and B-sites shows better agreement. This site occupancy is in good agreement with the site preference energy data [16]. Fig. 2a

represents the plot of lattice constant against composition x .

3.2. Transport studies

Fig. 3 shows the plot of logarithmic conductivity against inverse temperature for compounds $0 \leq x \leq 1$. All the conductivity data obeyed the Raschhiurichsen law $\sigma = \sigma_0 \exp(-Ea/kT)$. All graphs as shown, contain straight lines. It is clear from the plots that increasing the nickel content causes a decrease in activation energy. The plot shows no break or inflection, indicating the presence of the stable oxidation states of all the cations over temperature range studied. The values of the activation energy are listed in Table I and plotted in Fig. 2b. It is clear that the value of Ea slowly decreases from 0.707 to 0.373 eV with increasing doping of Ni^{2+} ion.

The plots of thermo-EMF ΔV developed across the compounds against the temperature difference ΔT are given in Fig. 4. The thermoelectric coefficient values vary between +740 and +136 $\mu\text{V K}^{-1}$ are listed in Table I and plotted in Fig. 2c.

The electrical conductivity σ is related to the total number of charge carriers P and their mobility at room temperature by the relation:

$$\sigma = Pe\mu \quad (2)$$

where e is the electric charge, P the number of holes per unit volume and μ the mobility of holes. The average unit cell volume is taken to be $(8.373)^3$. The value of hole concentration would be 10^{22} cm^{-3} , and mobility value is $10^{-9} \text{ cm}^2 \text{ V sec}^{-1}$. It has been also calculated using the formula of Heikes and Johnston

TABLE I Values of lattice constant a (nm), activation (Ea) and thermoelectric coefficient (α) for the system $\text{Zn}_{1-x}\text{Ni}_x\text{FeCrO}_4$

X	a (nm)	C (nm)	Ea (eV)	($\mu\text{V K}^{-1}$)
0.00	0.8393	0.8392	0.707	740
0.25	0.8385	0.8385	—	593
0.50	0.8374	0.8374	0.541	—
0.75	0.8364	0.8365	0.452	255
1.00	0.8353	0.8353	0.373	136

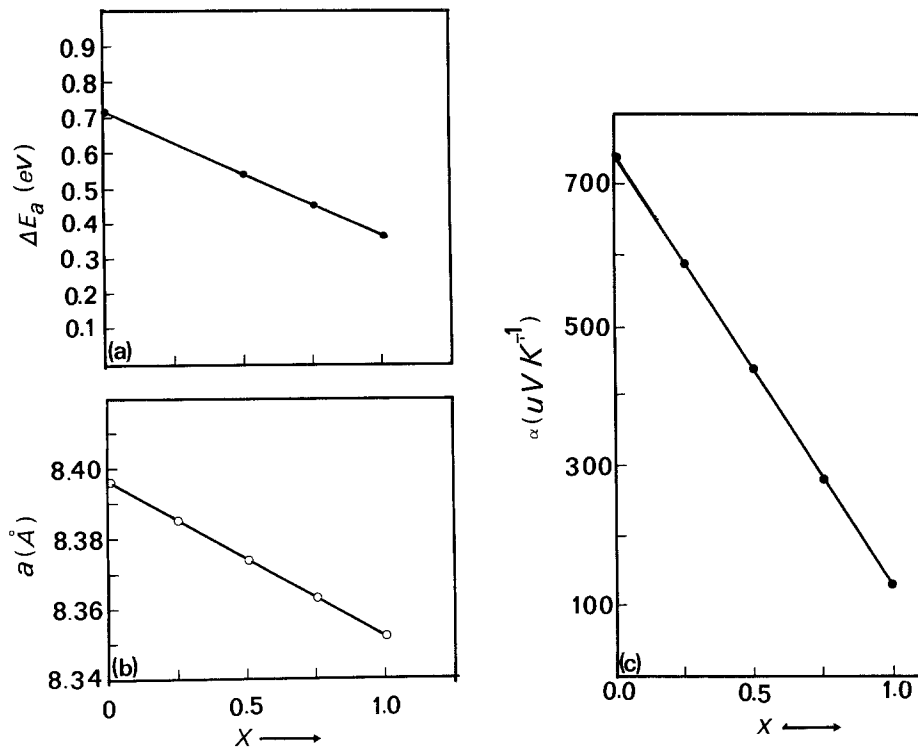


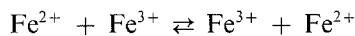
Figure 2 (a) Plot of lattice constant against composition. (b) Plot of activation energy against composition. (c) Plot of thermoelectric coefficient α against composition for the system $Zn_{1-x}Ni_xFeCrO_4$.

[17]

$$\mu = \left(\frac{ed^2\gamma}{kT} \right) \exp(-\Delta E/kT) \quad (3)$$

where d is the jump length of the charge carriers (taken as the average distance between neighbouring octahedral sites), calculated to be 3.0 nm using the normal procedure used by Jain and Darshane [18] and is the lattice frequency in the jumping process [19] and calculated to be 1.8×10^{13} Hz from the strong IR absorption band observed at 600 cm^{-1} . If ΔE is taken as average activation energy (0.518 eV) the mobility value is $10^{-9} \text{ cm}^2 \text{ V sec}^{-1}$. This reveals that all compounds possess a low mobility.

From Table I it is observed that all the compounds of the system are P-type semiconductors. The reason can be attributed to the loss of zinc oxide during the firing process creating vacancies at A-site. As a result a small amount of Fe^{3+} may go from B-site to A-site. Such probability has been suggested by Blase [20] and Lotgering [21]. The oxygen non-stoichiometry will give rise to some Fe^{2+} ions so as to maintain the electrical neutrality. Thus the following hopping mechanism is expected



Therefore, we have small polaron hopping charge

carriers. The presence of Fe^{2+} ions could not be detected by X-ray, however, very small concentrations of Fe^{2+} cannot be ruled out also.

3.3. Infrared spectra

Tarte and Preudhomme [22] and Tarte *et al.* [23] have observed that in ferrites, the absorption bands depend on the nature of octahedral cations and do not significantly depend on the nature of tetrahedral ions. However, Waldron [24] and Hafner [25] attributed the band at around 600 cm^{-1} to the intrinsic vibration of tetrahedral metal-oxygen complex and at around 400 cm^{-1} to the intrinsic vibration of octahedral complexes. The difference in band positions is because of difference in the $Fe^{3+}-O^{2-}$ distances for octahedral and tetrahedral complexes.

The presence of Fe^{2+} ions in the ferrites causes a shoulder or splitting of the absorption band [26]. In our compounds Fe^{3+} ions are present at both the sites. Neither of the bands show any shoulder nor splitting, indicating the absence of detectable Fe^{2+} ions.

4. Conclusion

Thus from X-ray electrical and IR studies we suggest the probable cation distribution for the system

TABLE II Comparison of intensity ratios for $Zn_{0.5}Ni_{0.5}FeCrO_4$ and $ZnFeCrO_4$

Cations at		I_{220}/I_{400}		I_{220}/I_{400}		I_{440}/I_{422}	
A-site	B-site	Observed	Calculated	Observed	Calculated	Observed	Calculated
$Zn_{0.5}Ni_{0.5}FeCrO_4$							
Zn^{2+}, Fe^{3+}	$Ni^{2+}, Fe^{3+}, Cr^{3+}$	0.727	0.725	0.336	0.336	2.589	2.590
Zn^{2+}, Ni^{2+}	Fe^{3+}, Cr^{3+}		2.022		0.727		1.283
$ZnFeCrO_4$							
Zn^{2+}	Fe^{3+}, Cr^{3+}	1.542	1.540	0.402	0.403	0.800	0.799
Fe^{3+}	Zn^{2+}, Cr^{3+}		2.014		0.489		1.545

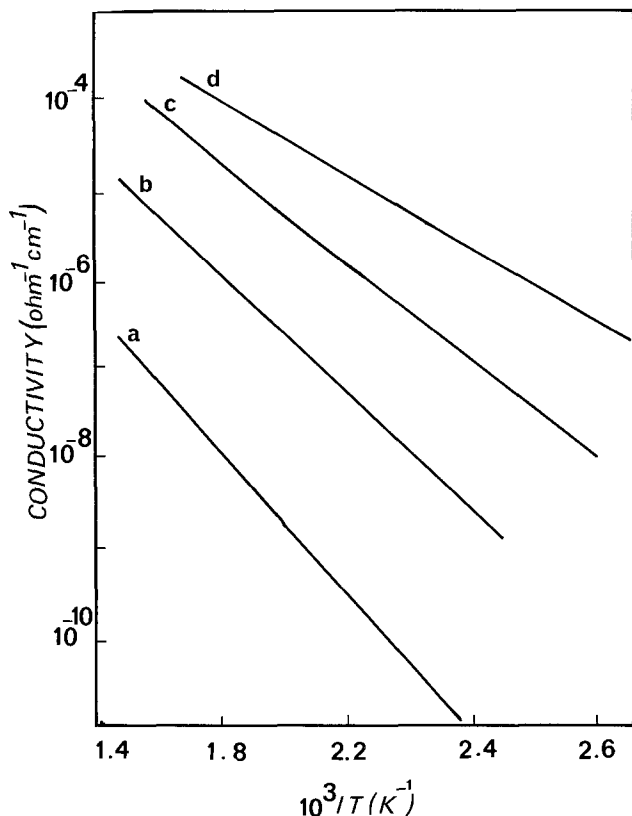


Figure 3 Plot of electrical conductivity against $10^3/T$ for the system $Zn_{1-x}Ni_xFeCrO_4$.

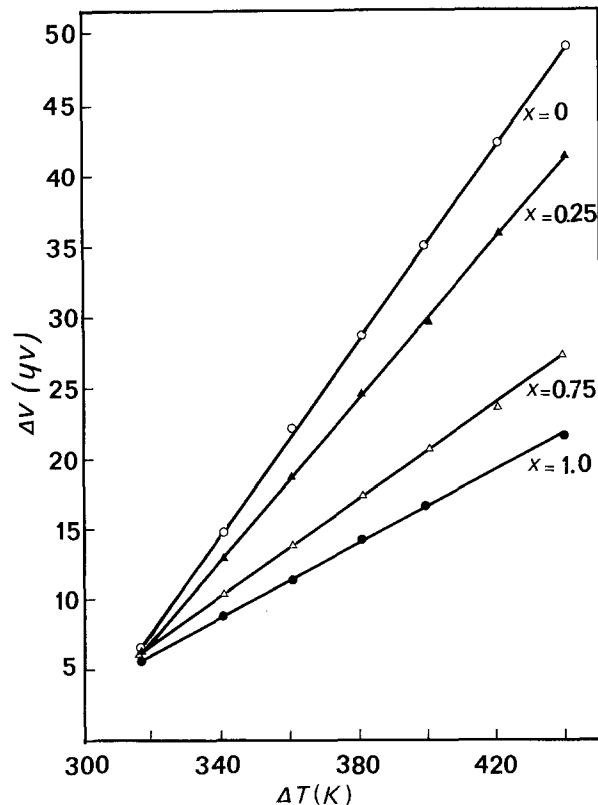
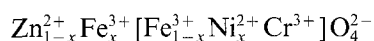


Figure 4 Plot of thermo e.m.f. (ΔV) against temperature for the system $Zn_{1-x}Ni_xFeCrO_4$.

$Zn_{1-x}Ni_xFeCrO_4$ to be as



References

- G. BLASE, *Philips Res. Rep. Suppl.* **3** (1964) 1.
- G. C. ULMER and W. J. SMOTHERS, *J. Amer. Ceram. Soc.* **51** (1968) 315.
- J. SMITH and H. P. J. WIJN, "Ferrites" (John Wiley, New York, 1959).
- D. G. WICKAM, *Inorg. Synth.* **9** (1967) 152.
- K. R. MANALOV, "Mathadicum Chemicum", Vol. 1, edited by K. Niedenzu and M. Zimmer (Academic Press, New York, 1976) p. 227.
- N. YAMAMOTO, S. KAWANO, N. ACHIWA, M. KIYAMA and T. TAKADA, *Jpn J. Appl. Phys.* **12** (1973) 1830.
- M. N. KHAN, S. AL-DALLAL and A. AHMED, Proceedings of the International Conference on "Effects of Modes of Formation on the Structure of Glass", Vanderbilt University, Nashville, Tennessee, U.S.A., June 16-20 1987.
- M. N. KHAN, A. AHMED and V. S. DARSHANE, *J. Mater. Sci.* **24** (1989) 163.
- Idem, ibid.* **24** (1989) 2615.
- M. J. BUERGER, "Crystal Structure Analysis" (Wiley, New York, 1960) p. 46.
- International tables for X-ray crystallography, Vol. 4 (Knoch Press, Birmingham, 1974) p. 72.
- L. WEIL, E. E. BERTAUT and L. BACHIROU, *J. Physique Radium* **11** (1950) 208.
- H. L. TULLER and A. S. NOWICK, *J. Phys. Chem. Solids* **38** (1977) 859.
- A. O. LES, *Phys. Status Solidi (A)* **3** (1970) 569.
- R. D. SHANNON and C. T. PREVITT, *Acta Cryst.* **B26** (1970) 1076.
- A. MILLER, *J. Appl. Phys. Suppl.* **30** (1959) 24.
- R. R. HEIKES and W. D. JOHNSTON, *J. Chem. Phys.* **26** (1957) 582.
- P. S. JAIN and V. S. DARSHANE, *Indian J. Chem.* **19A** (1980) 1050.
- P. TARTE, *Spectrochim. Acta.* **19** (1965) 49.
- G. BLASE, *J. Phys. Chem. Solids* **27** (1966) 383.
- F. K. LOTGERING, *J. Phys. Chem. Solids* **27** (1966) 139.
- P. TARTE and J. PREUDHOMME, *J. Acta. Crysta Uogr* **16** (1963) 227.
- P. TARTE and K. COLLONGUES, *Ann. Chim. Paris* **9C** (1964) 135.
- R. D. WALDRON, *Phys. Rev.* **99** (1955) 1727.
- S. HAFNER, *Z. Kristallogr.* **115** (1961) 331.
- V. R. K. MURTHY, S. CHITRA SANKAR, K. V. REDDY and J. SOBHANADRI, *Indian J. Pure Appl. Phys.* **16** (1978) 79.

Received 29 November 1988
and accepted 16 May 1989